



1 **Bi-directional air-sea exchange and accumulation of POPs (PAHs, PCBs, OCPs and**  
2 **PBDEs) in the nocturnal marine boundary layer**

3  
4 Gerhard Lammel<sup>1,2\*</sup>, Franz X. Meixner<sup>3</sup>, Branislav Vrana<sup>1</sup>, Christos Efstathiou<sup>1</sup>, Jiří  
5 Kohoutek<sup>1</sup>, Petr Kukučka<sup>1</sup>, Marie D. Mulder<sup>1</sup>, Petra Příbylová<sup>1</sup>, Roman Prokeš<sup>1</sup>, Tatsiana P.  
6 Rusina<sup>1</sup>, Guo-Zheng Song<sup>3</sup>, Manolis Tsapakis<sup>4</sup>

7  
8 <sup>1</sup>Masaryk University, Research Centre for Toxic Compounds in the Environment, Brno,  
9 Czech Republic

10 <sup>2</sup>Max Planck Institute for Chemistry, Multiphase Chemistry Dept., Mainz, Germany

11 <sup>3</sup>Max Planck Institute for Chemistry, Biogeochemistry Dept., Mainz, Germany

12 <sup>4</sup>Hellenic Centre for Marine Research, Institute of Oceanography, Gournes, Greece

13 \* lammel@recetox.muni.cz

14

15 **Abstract**

16 As a consequence of long-range transported pollution air-sea exchange can become a major  
17 source of persistent organic pollutants in remote marine environments. The vertical gradients  
18 in air of 14 species i.e., 4 parent polycyclic aromatic hydrocarbons (PAHs), 3 polychlorinated  
19 biphenyls (PCBs), 3 organochlorine pesticides (OCPs) and 2 polybrominated diphenylethers  
20 (PBDEs) in the gas-phase were quantified at a remote coastal site in the southern Aegean Sea  
21 in summer. Most vertical gradients were positive ( $\Delta c/\Delta z > 0$ ) indicating downward (net  
22 depositional) flux. Significant upward (net volatilisation) fluxes were found for 3 PAHs,  
23 mostly during day-time, and for 2 OCPs, mostly during night-time, as well as for 1 PCB and 1  
24 PBDE during part of the measurements. While phenanthrene was deposited, fluoranthene  
25 (FLT) and pyrene (PYR) seem to undergo flux oscillation, hereby not following a day/night  
26 cycle. Box modelling confirms that volatilisation from the sea surface has significantly



27 contributed to the night-time maxima of OCPs. Fluxes were quantified based on Eddy  
28 covariance. Deposition fluxes ranged  $-28.5 - +1.8 \mu\text{g m}^{-2} \text{d}^{-1}$  for PAHs and  $-3.4 - +0.9 \mu\text{g m}^{-2}$   
29  $\text{d}^{-1}$  for halogenated compounds. Dry particle deposition of FLT and PYR did not contribute  
30 significantly to the vertical flux.

31

## 32 **1. Introduction**

33 The marine atmospheric environment is a receptor for persistent organic pollutants (POPs)  
34 which are advected from sources on land, primary and secondary, such as volatilization from  
35 contaminated soils. This is a concern as these substance bioaccumulate along marine food  
36 chains (e.g., Lipiatou and Saliot, 1991; Borgå et al., 2001). Primary sources do not exist in the  
37 marine environment, except for polycyclic aromatic hydrocarbons (PAHs, ship engines).  
38 Long-range transport from urban and industrial sources on land are the predominant sources  
39 of PAHs and polychlorinated biphenyls (PCBs) in the global oceans (Atlas and Giam, 1986)  
40 and in the Mediterranean (Mandalakis et al., 2005; Tsapakis and Stephanou, 2005; Tsapakis  
41 et al., 2006; Iacovidou et al., 2009; Mulder et al., 2015).

42 However, the sea surface itself can turn into a secondary source of POPs provided  
43 concentrations build up in surface waters. Such studies are still rare. Re-volatilisation was  
44 observed for hexachlorocyclohexane (HCH) and PAHs, not only in coastal waters (Lohmann  
45 et al., 2011), but also in the open sea (Jantunen and Bidleman, 1995; Lakaschus et al., 2002)  
46 including the Mediterranean (Castro-Jiménez et al., 2012; Mulder et al., 2014). After long-  
47 term accumulation of declining emissions (even after phase-out), reversal of air-sea exchange  
48 may result at some point, as indicated by global modelling for organochlorine pesticides  
49 (OCPs; Stemmler and Lammel, 2009). The seasonality of on-going emissions on the other  
50 hand may trigger a seasonal reversal of air-sea exchange, as indicated for retene, a PAH  
51 emitted from biomass burning in the Mediterranean (summer maximum; Mulder et al., 2014).



52 Similarly, PAHs emitted in fossil fuel combustion in residential heating (winter maximum)  
53 may re-volatilise seasonally from the sea surface in receptor areas.

54 The direction of diffusive air-surface exchange flux of organics can be identified by  
55 comparing the fugacities and can be quantified based on the Whitman two-film model  
56 (Bidleman and Connell, 1995; Schwarzenbach et al., 2003) or micro-meteorological  
57 techniques. The latter have so far only rarely been used to quantify air-water (Perlinger et al.,  
58 2005; Rowe and Perlinger, 2012; Sandy et al., 2012; Wong et al., 2012) or air-soil (Parmele et  
59 al., 1972; Majewski et al., 1993; Kurt-Karakus et al., 2006) gas exchange fluxes.

60 We studied the vertical fluxes of POPs at sea surface level with a gradient method at a remote  
61 coastal site in the eastern Mediterranean. The measurements were done in the context of a  
62 coordinated multi-site campaign on POP cycling in the region (Lammel et al., 2015). The  
63 POP concentration in surface seawater was determined, too, such that the direction of air-sea  
64 exchange could be addressed by a second method.

65

## 66 **2.1 Site and sampling**

67 The site selected for atmospheric measurements was Selles Beach, at the northern coast of  
68 Crete, 35.2°N/25.4°E, very close (4 km) to the Finokalia observatory. This is a remote site,  
69 some 70 km east of major anthropogenic emissions (Iraklion, a city of 100000 inhabitants  
70 with airport and industries; Mihalopoulos et al., 1997; Kouvarakis et al., 2000). The  
71 Mediterranean region includes urban and industrial areas and is adjacent to source regions  
72 (i.e. western, central and eastern Europe). Exposure of the study area to long-range  
73 transported pollution from central and eastern Europe is highest in summer (Lelieveld et al.,  
74 2002).

75 Organic substances were collected 3-13 July in the gaseous and particulate atmospheric  
76 phases using low volume samplers ( $F \approx 2.3 \text{ m}^3 \text{ h}^{-1}$ , Leckel LVS,  $\text{PM}_{10}$  inlet) equipped with  
77 quartz fibre filter (QFF, Whatman QMA 47 mm, baked at 320°C prior to usage) and 2



78 polyurethane foam (PUF) plugs (Molitan, density  $0.030 \text{ g cm}^{-3}$ , 5.5 cm diameter, total depth  
79 10 cm, cleaned by extraction in acetone and dichloromethane, 8 h each) in series. Two of  
80 these samplers collected gases and particles at different heights (inlets at  $z_1 = 1.05$  and  $z_2 =$   
81 2.8 m), about 0.5 m apart in the horizontal. Day-time (9-20 h EEDST) and night-time (21-8 h  
82 EEDST) sampling was conducted from 2 July in the evening until 13 July 2012 in the  
83 evening. During part of the measurements, from 6 July in the morning until 10 July 2012 in  
84 the evening, a third sampler was used to collect replica of gaseous samples (PUF plugs only)  
85 at  $z_1$ . For the concentration at  $z_1$ ,  $c_{z1}$ , replica concentrations (mean of 2 measurements) were  
86 used whenever possible. The samplers were placed on a rocky beach. The horizontal distance  
87 between the samplers and the water was  $\approx 3$  m, while the vertical distance between the rock  
88 and water surfaces was 0.1-0.3 m, varying due to tide and waves. After exposure, filters and  
89 PUFs were packed in Al foil and zip-bags, stored and transported in a cool box to the  
90 laboratory.

91 Free dissolved contaminants in seawater were sampled using silicone rubber (SR) sheets  
92 (Altec, Great Britain) as passive water samplers (PWS). Quantification of trace organics from  
93 PWS is sensitive and validated (Rusina et al., 2010). Uncertainties in results obtained by  
94 application of partition based passive samplers are believed to range around a factor of two  
95 depending on the level of experience of the laboratory (Allan et al., 2009). Different aspects  
96 of uncertainty are discussed in Lohmann et al. (2012). At two localities, distanced 0.8 and 2.2  
97 km west of Selles Beach, each two SR PWS were deployed in parallel. Each sampler  
98 consisted of six sheets ( $55 \times 90 \times 0.5$  mm). Before exposure SR sheets were cleaned by  
99 Soxhlet extraction in ethyl acetate (96 h) followed by methanol (48 h, shaken), and spiked by  
100 a mix of 15 performance reference compounds (PRCs; D<sub>10</sub>-biphenyl and 13 PCB congeners  
101 not occurring in the environment) according to the procedure (Booij et al., 2002). Samplers  
102 were deployed 3 July – 2 August 2012 in water mounted on stainless steel wire holders at 1 m



103 depth using buoy and rope. After exposure, samplers were stored and transported in original  
104 vials and brought in a cool box to the laboratory.  
105 Daily mean temperature was 28.2 (22.4-34.5)°C and wind velocity was 4.8 (0.6-7.7) m s<sup>-1</sup>  
106 (hourly data). No precipitation occurred. The meteorological situation is described in the  
107 Supplementary information (SI), S2.1.

108

## 109 **2.2 Meteorological parameters and vertical flux calculations**

110

111 Boundary layer (BL) depth is needed for interpretation of the variation of the concentrations  
112 in air. BL depth data are taken from simulations of the Lagrangian dispersion model  
113 FLEXPART, version 9 (Stohl et al., 1998). These were run in forward direction, and based on  
114 analysed wind fields (ECMWF, 0.5° resolution). The model BL height is calculated according  
115 to Vogelesang and Holtslag (1996) using the critical Richardson number. According to wind  
116 direction during sampling we allocate BL depths at upwind locations well off shore (70-100  
117 km) or inland (≈20 km), respectively, as the relevant BL depth for interpretation of  
118 atmospheric concentrations at the coastal site. The mean BL depth during sampling intervals  
119 is used.

120 For characterization of the local meteorological conditions, continuous measurements (5 min  
121 averages) of air temperature, relative humidity, wind speed and wind direction were accom-  
122 plished by three automatic weather stations (model WMT520; Vaisala, Helsinki, Finland)  
123 which have been placed at the beach in ≈200 m distance (2) and ≈100 m inland (1),  
124 respectively, from the sampling location. For characterization of the atmospheric surface  
125 layer's thermodynamic stratification, vertical profiles of wind speed, wind direction, air tem-  
126 perature and relative humidity were determined by continuous measurements at four levels  
127 (0.34, 0.70, 1.45, and 3.00 m above ground). Data was recorded by 2D ultrasonic wind  
128 sensors (model WMT701; Vaisala, Helsinki, Finland) and aspirated temperature and relative



129 humidity sensors (model MP103A; Rotronic, Bassersdorf, Switzerland) in 10 s intervals,  
130 which were averaged to 30 min means for further data processing. For determination of key  
131 micrometeorological quantities (e.g., sensible heat flux, friction velocity; see SI, S1.3), fast  
132 response measurements of the 3D wind vector and air temperature have been performed by a  
133 3D ultrasonic anemometer (CSAT-3, Campbell Scientific Inc., Logan, USA) on a small mast,  
134 4 m above ground and about 7 m ESE of the profile mast. Corresponding data were  
135 continuously recorded with a sampling frequency of 20 Hz by a suitable logger (model  
136 CR3000; Campbell Scientific Inc., Logan, USA). Key micrometeorological quantities were  
137 derived from fast response 3D wind and air temperature data (20 Hz) according to the eddy  
138 covariance (EC) method; 20 Hz data were processed by the TK3 algorithm (Mauder and  
139 Foken, Department of Micrometeorology, University of Bayreuth, Germany), and the results  
140 were averaged every 30 minutes. Only periods with wind direction between 270° and 40°  
141 (i.e., onshore winds) were considered to calculate vertical fluxes of gaseous organics (more  
142 details in the SI, S2.1).

143 The turbulent vertical gaseous organics flux,  $F_c$  ( $\text{ng m}^{-2} \text{s}^{-1}$ ), has been calculated according to  
144 the aerodynamic method as the product of the vertical difference of concentration,  $\Delta c_z$  ( $\text{ng m}^{-3}$ ), and the turbulent transfer velocity,  $v_{\text{tr}}$  ( $\text{m s}^{-1}$ ):

$$146 \quad F_c = -v_{\text{tr}} \Delta c_z = -v_{\text{tr}} [c(z_2) - c(z_1)]$$

147

148 where  $z_2$  and  $z_1$  are the heights of inlets of gaseous organics' sampling (1.05 m and 2.80 m,  
149 see 2.1, above). The transfer velocity is a measure of the vertical turbulent (eddy) diffusivity.  
150 Details of the underlying formulation and the calculation scheme are given in the SI, S1.3.

151

## 152 **2.3 Chemical analysis**



153 For organic analysis all samples were extracted with dichloromethane during  $\approx 1$  h in an  
154 automatic extractor (Büchi B-811). Surrogate extraction standards ( $D_8$ -naphthalene,  $D_{10}$ -  
155 phenanthrene,  $D_{12}$ -perylene, PCB30, PCB185,  $^{13}C$  BDEs 28, 47, 99, 100, 153, 154, 183 and  
156 209) were spiked on each PUF and QFF prior to extraction. The volume was reduced after  
157 extraction under a gentle nitrogen stream at ambient temperature, and fractionation was  
158 achieved on a silica gel column. Samples were analyzed using a GC-MS (gas chromatograph  
159 coupled with a mass spectrometer) Agilent 7890 coupled to Agilent 7000B with a J&W  
160 Scientific fused silica column DB-5MSUI (60 m  $\times$  0.25 mm  $\times$  0.25  $\mu$ m) for 2-4-ring PAHs  
161 (naphthalene (NAP), acenaphthylene (ACY), acenaphthene (ACE), fluorene (FLN),  
162 phenanthrene (PHE), anthracene (ANT), fluoranthene (FLT), pyrene (PYR),  
163 benzo(a)anthracene (BAA), and chrysene (CHR). Terphenyl was used as injection standard.  
164 The temperature program was 80°C, 15°C min<sup>-1</sup> to 180°C, 5°C min<sup>-1</sup> to 310°C. The injection  
165 volume was 1  $\mu$ L in splitless mode at 280°C, with He used as a carrier gas at constant flow of  
166 1.5 mL min<sup>-1</sup>.

167 A sulphuric acid modified silica gel column was used for the PCB/OCP and PBDE cleanup.  
168 Samples were analyzed using a GC-MS/MS Agilent 7890 coupled to Agilent 7000B with a  
169 SGE HT-8 column (60 m  $\times$  0.25 mm  $\times$  0.25  $\mu$ m) for  $\alpha$ -HCH,  $\beta$ -HCH,  $\gamma$ -HCH,  $\delta$ -HCH, *o,p'*-  
170 and *p,p'*-DDE, -DDD and -DDT, penta- and hexachlorobenzene (PeCB, HCB). PCB 121 was  
171 used as injection standard for chlorinated substances. The temperature program was 80°C (1  
172 min hold), 40°C min<sup>-1</sup> to 200°C, 5°C min<sup>-1</sup> to 305°C. The injection volume was 3  $\mu$ L in  
173 splitless mode at 280°C, with He used as a carrier gas at constant flow of 1.5 mL min<sup>-1</sup>.

174 PBDEs were analysed using GC-HRMS (gas chromatography with high resolution mas  
175 spectrometry) on a Restek RTX-1614 column (15 m  $\times$  0.25 mm  $\times$  0.1  $\mu$ m). The resolution  
176 was set to > 10000 for BDE 28–183, and > 5000 for BDE 209.  $^{13}C$  BDEs 77 and 138 were  
177 used as injection standards. The MS was operated in EI+ mode at the resolution of >10000.  
178 The temperature program was 80°C (1 min hold), then 20°C min<sup>-1</sup> to 250°C, followed by



179 1.5°C min<sup>-1</sup> to 260°C and 25°C min<sup>-1</sup> to 320°C (4.5 min hold). The injection volume was 3 µL  
180 in splitless mode at 280°C, with He used as a carrier gas at constant flow of 1 mL min<sup>-1</sup>.

181

182 Recovery of native analytes varied between 72 and 102% for PAHs, between 88 and 103%  
183 for PCBs, and between 75 and 98% for OCPs. The results for PAHs, OCPs and PCBs were  
184 not recovery corrected. For PBDEs, isotopic dilution method was used, the average recoveries  
185 ranged 78-128%.

186 The mean of 4 field blank values was subtracted from the air sample values. Values below the  
187 mean + 3 standard deviations of the field blank values were considered to be <LOQ. Field  
188 blank values of most analytes in air samples were below the instrument limit of quantification  
189 (ILOQ), which corresponded to 6-34 pg m<sup>-3</sup> for PAHs, 7-23 pg m<sup>-3</sup> for PCB and OCPs and  
190 0.003-0.04 pg m<sup>-3</sup> for PBDEs (SI, Table S2). Higher LOQs were determined for analytes in  
191 gaseous air samples, namely 0.18 and 0.50 ng m<sup>-3</sup> for FLN and PHE, and typically 28 pg m<sup>-3</sup>  
192 for HCB. In the particulate phase a higher LOQ resulted for PHE, i.e. 170 pg m<sup>-3</sup>. The  
193 breakthrough in PUF samples was estimated, and as a consequence, NAP, FLN, HCB and  
194 PeCB results are not considered as the sampled air volume (typically ≈25 m<sup>3</sup> for PUFs)  
195 expectedly lead to breakthrough under the prevailing temperatures (Melymuk et al., 2016).

196 Free dissolved water concentrations of analytes in PWS were calculated from amounts  
197 accumulated in SRs using the exponential uptake model described in Smedes (2007). The  
198 required sampling rates were estimated by fitting performance reference compounds  
199 dissipation data from sampler to the model described by Booij and Smedes, 2010. ILOQ  
200 corresponded to 0.5-4.2 pg L<sup>-1</sup> for PAHs (but 9 pg L<sup>-1</sup> for NAP), 0.05-0.5 pg L<sup>-1</sup> for PCB and  
201 OCPs and 0.0003-0.037 pg L<sup>-1</sup> for PBDEs (SI, Table S2). Site specific LOQs were 1–10 pg L<sup>-1</sup>  
202 <sup>1</sup> for PAHs (but 400 pg L<sup>-1</sup> for NAP), 0.1-0.8 pg L<sup>-1</sup> for PCB, 0.1–1.4 pg L<sup>-1</sup> for OCPs (but 2.8  
203 pg L<sup>-1</sup> for α-HCH) and 0.01–0.11 pg L<sup>-1</sup> for PBDEs (but 0.59 pg L<sup>-1</sup> for BDE209).

204





#### 205 **2.4 Vertical gradients of trace organics' concentration in air**

206 Air-sea gas exchange can be studied by determining the vertical concentration gradients of  
207 trace gases in air (Doskey et al., 2004; Else et al., 2008).

208 Three standard deviations of field blank concentrations are considered as the absolute  
209 uncertainty of concentration measurements,  $c$ , and twice that much as the uncertainty of  
210 concentration differences,  $\Delta c_z$ . Values of concentrations and vertical concentration differences  
211 (gradients) not exceeding these thresholds are considered insignificant. This applied for a  
212 large fraction of gradients, namely OCP (34 out of 70), PCB (27 out of 44), PBDE (4 out of  
213 5), and PAHs (17 out of 46) (Table S3).

214

#### 215 **2.5 Air-water fugacity ratio**

216 The direction of diffusive air-sea gas exchange can be derived from the fugacity ratio  
217 calculation, based on the Whitman two-film model (Bidleman and McConnell, 1995). The  
218 fugacity ratio,  $f_a/f_w$ , is calculated as:

219

$$220 f_a/f_w = c_a R T_a / (c_w H_{T_w, salt})$$

221

222 with gas-phase concentration  $c_a$  ( $\text{ng m}^{-3}$ ), dissolved aqueous concentration  $c_w$  ( $\text{ng m}^{-3}$ ),  
223 universal gas constant  $R$  ( $\text{Pa m}^3 \text{ mol}^{-1} \text{ K}^{-1}$ ), sea surface temperature (SST),  $T_w$ , and both  $T_w$   
224 and salinity corrected Henry's law constant  $H_{T_w, salt}$  ( $\text{Pa m}^3 \text{ mol}^{-1}$ ; see S1.1 for details), and air  
225 temperature  $T_a$  (K).  $T_a$  was adopted from the on-site measurement (see above).  $c_w$  is derived  
226 as the average of the results at two localities, 2 replicas each (see above, 2.1). SST data,  
227 measured on the sampling day and in the area, were downloaded from respective database  
228 (see S1.4 for details). Air and water sampling was not totally in phase: sampling in air was  
229 over 12 days (2-13 July), while SR exposure was during 28 days (3-30 July) i.e., collection  
230 was done 10 days after air sample collection. Consequently, for those substances which are



231 quickly equilibrated (within a few days) in PWS i.e., HCH and 3-ring PAHs, no simultaneous  
232 measurement in air and water was done (see section 2.1). Although the seawater  
233 concentrations of HCH and 3-ring PAHs might have been stable over 28 days, no such  
234 evidence exists and we refrain from relating the fugacities. Values  $0.3 < FR < 3.0$  are  
235 conservatively considered to not safely differ from phase equilibrium, as propagating from the  
236 uncertainty of the Henry's law constant,  $H_{T_w, salt}$ , and measured concentrations and  
237 temperature changes during sampling (e.g., Bruhn et al., 2003; Castro-Jiménez et al., 2012).  
238 Substance property data are taken from the literature (SI, Table S1). This conservative  
239 uncertainty margin is also adopted here, while  $f_a/f_w > 3.0$  indicates net deposition and  $f_a/f_w$   
240  $< 0.3$  net volatilisation.

241

## 242 **2.6 Non-steady state 2-box model**

243 The air–sea mass exchange flux of several OCPs and PAHs are simulated by a non-steady  
244 state zero-dimensional model of intercompartmental mass exchange (Lammel, 2004; Mulder  
245 et al., 2014) in order to test the hypothesis that the diurnal variation of contaminant  
246 concentrations in air during a period of on-shore advection of one air mass is explained by the  
247 combination of volatilisation from the sea surface and atmospheric mixing depth, while  
248 advection (long-range transport) is less significant (horizontal homogeneity of air mass;  
249 Lammel et al., 2003). This 2-box model predicts concentrations by integration of two coupled  
250 ordinary differential equations that solve the mass balances for the two compartments, namely  
251 the atmospheric marine BL and seawater surface mixed layer. Processes considered in air are  
252 dry (particle) deposition, removal from air by reaction with the hydroxyl radical, and air-sea  
253 mass exchange flux (dry gaseous deposition), while in seawater export (settling) velocity,  
254 deposition flux from air, air-sea mass exchange flux (volatilisation), and degradation (as first  
255 order process) are considered. Input parameters are listed in the SM, Table S3.

256



## 257 **3. Results and discussion**

### 258 **3.1 Day/night variation of concentrations in air**

259 4 PAHs (ACE, PHE, FLT, PYR), 3 OCPs ( $\alpha$ - and  $\gamma$ -HCH, *p,p'*-DDE), 3 PCB congeners  
260 (PCB28, -52 and -101) and 2 PBDE congeners (BDE47 and -99) were quantified in gas-phase  
261 samples, while the other species were found <LOQ in all or most samples (Fig. 1a, 2a, Table  
262 1a, b). This is a consequence of limited air sample volume ( $\approx 25$  m<sup>3</sup>). PAHs and PBDEs were  
263 also found in the particulate phase. The levels observed (Table 1a) are at the lower end of  
264 what had been reported from marine, rural and remote sites in the region in the previous  $\approx 15$   
265 years, in particular with regard to the chlorinated species (Kamarianos et al., 2002;  
266 Mandalakis and Stephanou, 2002; Tsapakis and Stephanou, 2005; Cetin and Odabasi, 2008;  
267 Halse et al., 2011; Lammel et al., 2010 and 2011; Castro-Jiménez et al., 2012; Berrojalbiz et  
268 al., 2014; Mulder et al., 2014 and 2015). To our best knowledge, the DDE levels are the  
269 lowest reported from the region. This confirms the remote character of the site. Influence of  
270 local sources, not expected at this remote site (Iacovidou et al., 2009), is sometimes indicated  
271 by an anti-correlation between wind speed and atmospheric concentration. At Selles Beach,  
272 dilution by higher wind speed is indeed indicated for one contaminant, ACE (by significant  
273 anti-correlation,  $p < 0.05$  confidence level, t-test). This is expected, because of its short  
274 atmospheric lifetime.

275 BL depths ranged 160-500 m during night-time and 270-760 m during day-time (mean of  
276 sampling intervals i.e., 11 h). Day/night variation of contaminants' atmospheric  
277 concentrations, often related to mixing and local sources, was not obvious: For PAHs the  
278 mean ratio of day/night concentrations  $c_{\text{day}}/c_{\text{night}} = 0.67$  for ACE, while it was  $c_{\text{day}}/c_{\text{night}} = 1.4$ -  
279 1.55 for PHE, FLT and PYR. Also for PBDEs  $c_{\text{day}}/c_{\text{night}} > 1$  is found (1.20 and 1.37). The low  
280 value for ACE can be explained by its short photochemical lifetime (Keyte et al., 2013).  
281  $c_{\text{day}}/c_{\text{night}} > 1$  was previously observed for PAHs at the same site and explained by temperature



282 driven volatilisation from surfaces overcompensating for photochemistry (Lee et al., 1998;  
283 Tsapakis and Stephanou, 2007). For chlorinated substances, we find  $c_{\text{day}}/c_{\text{night}} < 1$ , namely  
284 0.56-0.66 for HCH isomers, and 0.68-0.95 for PCBs and DDE. However, there was a clear  
285 day/night, with mostly night-time maxima trend during a period of continuous on-shore  
286 winds, 6-10 July (Fig. 1). Apparently, contaminants' concentrations were influenced by BL  
287 depth, as indicated by anti-correlation with PAHs and OCPs (except DDE; significant for  $\alpha$ -  
288 HCH on the  $p < 0.05$  confidence level, t-test). This, apart from mixing, is related to advection  
289 and air-sea mass exchange and studied in more detail in Section 3.5.

290

### 291 **3.2 Diffusive air-sea exchange**

292 The variation of air concentrations (with nighttime maxima) during a period of northerly flow  
293 without change of air mass is predicted using the 2-box model (Section 2.6). For PCB28, -52,  
294 FLT and BDE47 air concentrations are qualitatively well captured (Fig. 2, S4). These are  
295 maintained by dry gaseous deposition alone (PCB52, FLT) or by oscillating fluxes (HCB,  
296 PCB28: mostly upward, PYR: mostly downward; Fig. S5). The model predicted fluxes are in  
297 good agreement with the observed values (Section 3.3, Table S5) except for each one day-  
298 time sampling interval of FLT and BDE47 (upward fluxes), and for one day-time interval of  
299 PCB28 (downward flux; in total 4 agreements, 3 disagreements). The modelling results  
300 support that (during advection of one air mass) the diurnal variation of contaminant  
301 concentrations in air was explained by the combination of volatilisation from the sea surface  
302 and atmospheric mixing depth. Volatilisation from the sea surface has significantly  
303 contributed to the night-time maxima of HCB and PCB28, as well as of PYR during 1 night  
304 (night-time upward fluxes; Table S5). This, to our knowledge, had never been observed  
305 before.

306  $f_w$  is derived from the mean concentrations in seawater at two locations (see SI, Table S6, for  
307 individual data). The comparison of air-water fugacity ratios (Section 2.5) suggests for the



308 measurement period, 2-13 July 2012, net deposition (prevailing downward fluxes,  $f_a/f_w > 3$ ) of  
309 gaseous FLT, PYR, BDE47 and -99, net volatilization (prevailing upward fluxes,  $f_a/f_w < 0.3$ )  
310 of gaseous PCB28 and -101 and close to phase equilibrium ( $0.3 < f_a/f_w < 3$ ) for *p,p'*-DDE,  
311 and PCB52 (Table 2). These results are the same as determined based on passive air sampling  
312 at several locations along the shore at and near Selles Beach (Lammel et al., 2015).  
313 The direction of DDE and PCB fluxes derived from fugacity calculations is consistent with  
314 what was indicated by the correlation of air concentrations and BL depth during on-shore  
315 winds (SI, S2.5).

316

### 317 **3.3 Vertical concentration gradients in air**

318 PAH vertical gradients mostly indicated deposition,  $\Delta c/\Delta z > 0$ , found in 28 cases (14 during  
319 day, 14 during night), while negative gradients were found in 10 cases (8 during day, 2 during  
320 night). The vertical gradient of PAHs was insignificant in 17 cases. When volatilisation was  
321 observed (3-5 July for FLT and PYR, 6-9 July for ACE)  $\Delta c/\Delta z$  tended to be clearly lower  
322 during day-time, indicating that volatilisation of PAHs from the sea surface was stronger  
323 during day-time. This could be explained by a higher fugacity from seawater,  $f_w$ , which  
324 increases with  $H_{T_w, salt}$  (see above, 2.5), which, in turn, increases with sea surface temperature,  
325  $T_w$ . Similarly, for the halogenated substances, significant positive gradients,  $\Delta c/\Delta z > 0$ ,  
326 indicating deposition were more frequent than significant negative gradients i.e., 37 cases (15  
327 PCBs, 22 OCPs, 30 during day, 7 during one night only) and 20 cases (2 PCBs, 17 OCPs, 1  
328 PBDE, 5 during day, 15 during night), respectively. For these substance classes, a vertical  
329 gradient was insignificant in 65 cases (according to the measurement uncertainties). During at  
330 least some nights of the period 6-10 July night-time maxima of HCH, and PCB52 in air  
331 coincided with negative vertical gradients, i.e. emissions from the sea surface. This trend is  
332 most significant for the HCH isomers for which a stronger volatilisation flux from the sea



333 surface is found during the nights than during day time ( $\Delta c/\Delta z < 0$ ), or even deposition during  
334 day-time ( $\Delta c/\Delta z > 0$  on 6 and 9 July). Hence, volatilisation from the sea surface may have  
335 contributed to and may even have caused the night-time maxima of the atmospheric  
336 concentrations of HCH and PCB52 (see above and Table 1a): The diel variation of air  
337 temperature was small i.e., day-time mean was typically 0.5-1.5 K warmer than night-time  
338 mean temperature. Even somewhat lower upward fluxes,  $F_c$ , of HCH during night than during  
339 day, caused by a slightly lower sea surface temperature, may have caused  $c_{\text{day}}/c_{\text{night}} < 1$  in  
340 combination with the day/night variation of the BL depth (by average 50% deeper for day-  
341 time sampling periods). PBDE day-time maxima may indicate local volatilisation from soil,  
342 enhanced during day-time. Again, this is consistent with the positive correlation of air  
343 concentrations with BL depth (above). Only one BDE concentration gradient was significant,  
344 which was volatilisational and during day-time (Fig. 1b, Table 1b). Fluctuating PCB fluxes  
345 are in line with the observation that PCBs were close to phase equilibrium in the Aegean in  
346 2006 (Berrojalbiz et al., 2014). Summarizing, average significant day-time vertical gradients,  
347  $\Delta c/\Delta z$ , of all contaminants exceeded average significant night-time gradients, except for FLT  
348 and PYR.

349 The direction of the gradient, hence, of air-sea exchange is found to have changed for ACE,  
350 PYR and the HCH isomers on a half-day basis (sequential sampling periods), for FLT during  
351 less than 2 days (Table S4). Changing directions of net air-sea mass exchange had been  
352 observed in the region along a ship cruise for OCPs, PCBs and one alkylated PAH,  
353 dimethylphenanthrene (Castro-Jiménez et al., 2012; Berrojalbiz et al., 2014) in 2006 and for  
354 FLT and PYR in 2010 (Mulder et al., 2014). Fast fluctuation of the direction of air-sea  
355 exchange throughout large parts of the year had been found for one alkylated PAH, retene, in  
356 the sea region following biomass burning emissions (based on box modelling; Mulder et al.,  
357 2014). Earlier, in 2000-02 air-sea exchange of PAHs was found depositional for all members  
358 (Tsapakis et al., 2006).



359 These observations of an increasing number of pollutants attaining phase equilibrium and bi-  
360 directional flux may indicate a long-term trend from deposition towards ‘reversal’, i.e.  
361 volatilisation of these pollutants in the marine environment of the eastern Mediterranean and,  
362 more general, of receptor seas regions, located in the outflow of regions emitting long-lived  
363 semivolatile pollutants, such as most POPs. For substances close to phase equilibrium  
364 (attained in a long-term trend) the direction of air-sea exchange may change with a high  
365 frequency, as found here. However, fluctuation may also occur in response to seasonal trends:  
366 In summer 2010 FLT and PYR were found close to phase equilibrium in the eastern  
367 Mediterranean, while retene (RET) was found mostly volatilisational. A model simulation had  
368 revealed that seasonal primary emissions and subsequent deposition of RET (from open fires  
369 in the region) are triggering seasonal flux reversal, which over many weeks, however, is  
370 fluctuating with a high frequency (< 24 h). (Mulder et al., 2014) Obviously, longer  
371 observations are needed to assess the prevailing vertical flux direction. Extrapolation of the  
372 observations to annual fluxes is not justified, as day/night fluctuations may be part of a more  
373 complex temporal pattern. The seawater surface as secondary source of pollution should be  
374 assessed based on flux measurements during several seasons and over longer time periods.

375

### 376 **3.4 Quantification of vertical fluxes of gaseous contaminants**

377 Vertical fluxes,  $F_c$ , can be quantified for periods with transfer velocity,  $v_{tr}$ , determined, which  
378 varied between 3.3 and 8.4  $\text{cm s}^{-1}$ , by average it was  $5.3 \pm 1.9 \text{ cm s}^{-1}$ . The time coverage of this  
379 parameter was 70%, however, i.e., satisfying time coverage of sampling intervals was  
380 achieved during 14 out of 20 sampling intervals, 11 days (by average  $5.5 \text{ cm s}^{-1}$ ) and 3 nights  
381 (by average  $3.5 \text{ cm s}^{-1}$ ) (Figures 1a, 2c, Table S5).

382 The fluxes of PAHs could be determined based on 8 periods of day-time and 2 periods of  
383 night-time sampling. 15 PAH fluxes were downward ( $F_c = -3.6 \pm 7.0 \mu\text{g m}^{-2} \text{ d}^{-1}$ ), 8 upward  
384 (ranging  $F_c = 0.8 \pm 0.6 \mu\text{g m}^{-2} \text{ d}^{-1}$ ) and insignificant ( $|F_c| < (0.7 \pm 0.7) \mu\text{g m}^{-2} \text{ d}^{-1}$ ) in 13 cases.



385 Both directions were observed for 3 species, while the flux of PHE was downward (by  
386 average  $F_c = -7.3 \mu\text{g m}^{-2} \text{d}^{-1}$ ) whenever significant (Table S5a). With

387

$$388 \quad v_{\text{dep}} = -F_c / c_g,$$

389

390 this corresponded to a mean deposition velocity for gaseous PHE of  $v_{\text{dep}} = 0.0043 \pm 0.0031 \text{ cm}$   
391  $\text{s}^{-1}$ , still significantly deviating from zero. Even 3-ring PAHs' deposition is dominated by the  
392 particulate phase and a wide range has been reported ( $0.001\text{-}10 \text{ cm s}^{-1}$ ; Zhang et al., 2015),  
393 also based on measurements in the region (Tasdemir and Esen, 2009). During the first days of  
394 the campaign FLT and PYR were volatilised, later deposited, too.

395 For 11 periods of day-time and 2 of night-time sampling the fluxes of 8 halogenated  
396 substances were downward in 12 cases ( $F_c = -0.58 \pm 0.87 \mu\text{g m}^{-2} \text{d}^{-1}$ ), upward in 6 cases ( $F_c =$   
397  $0.30 \pm 0.31 \mu\text{g m}^{-2} \text{d}^{-1}$ ; these were  $0.11\text{-}0.25$  for  $\gamma$ -hexachlorocyclohexane (HCH) and  $0.91 \mu\text{g}$   
398  $\text{m}^{-2} \text{d}^{-1}$  for BDE47) and insignificant in 15 cases ( $|F_c| \lesssim 0.19 \pm 0.45 \mu\text{g m}^{-2} \text{d}^{-1}$ ) (Table S5b).

399 The fluxes corresponded to mean deposition velocities not distinguishable from zero e.g.,  
400  $0.020 \pm 0.032 \text{ cm s}^{-1}$  for  $\alpha$ -HCH and  $0.011 \pm 0.015 \text{ cm s}^{-1}$  for PCB28.

401 Air-sea exchange fluxes had been estimated earlier based on measurements in air and  
402 seawater in the Aegean Sea and application of the 2-film model for PAHs in 2001-02  
403 (Tsapakis et al., 2006) and in spring 2006 for PAHs, HCB and PCBs (Castro-Jiménez et al.,  
404 2012). Hereby, the flux is calculated proportional to a substance specific mass transfer  
405 coefficient,  $k_{ol}$ , strongly dependent on wind velocity and sea surface temperature (Jurado et  
406 al., 2004; Mandalakis et al., 2005). For both PCBs and PAHs widely varying  $k_{ol}$  values have  
407 been estimated (Gigliotti et al., 2002; Mandalakis et al., 2005). The corresponding mean  $F_c$  (5  
408 sampling periods, just 1 in the case of ACE; Table S5) found in our study, 2012, has the same  
409 direction but exceeds by more than one and two orders of magnitude, respectively, the  
410 previous findings for PHE (downward) and FLT (downward in 2001-02, upward in 2006). For





411 PYR the opposite direction (now upward, downward in 2001-02 and 2006) is found. The flux  
412 direction found for the PCBs is unchanged compared to the 2006 measurements, then found  
413 close to phase equilibrium (Berrojalbiz et al., 2014).

414

### 415 **3.5 Particulate phase concentrations and total deposition**

416 Only PAHs and PBDEs were found exceeding LOQ in the particulate phase. Their day-night  
417 variation was minimal (Table S3a, b), by average  $c_{\text{day}}/c_{\text{night}} = 0.90\text{-}1.18$  for particulate PAHs,  
418 1.03 and 1.07 for the PBDEs. This supports the perception that particulate PAH is not  
419 attacked by the hydroxyl radical, but 'shielded' by the particle matrix (e.g. Zhou et al., 2012).  
420 The same had been observed previously at the same site (Tsapakis and Stephanou, 2007).  
421 Effective photochemistry can also be excluded for particulate PBDEs for the same  
422 reason. While  $c_{\text{day}}/c_{\text{night}} = 1.20$  and 1.37 for gaseous PBDEs suggests volatilisation from ground  
423 during the day, the absence of  $c_{\text{day}}/c_{\text{night}} > 1$  for the particulate phase may indicate that the  
424 species are not in gas-particle phase equilibrium. This has been pointed out based on previous  
425 PBDE measurements in the region (Cetin and Odabasi, 2008). However, the data set  
426 discussed here is limited and gas-particle partitioning was not the subject of this study.

427 Total deposition is the sum of dry and wet deposition, the latter not being significant in the  
428 Mediterranean in summer. Dry deposition is the sum of particle deposition and diffusive  
429 depositional fluxes (part of air-sea exchange, see 3.2). The dry particle deposition flux,  $F_{p \text{ dep}}$ ,  
430 can be estimated based on

431

$$432 F_{p \text{ dep}} = -v_{\text{dep}} c_p$$

433

434 with  $v_{\text{dep}}$  being determined by particle size and wind speed. Dry particle deposition to the sea  
435 surface is most efficient under high wind speeds (Williams, 1982). The mass median diameter  
436 of PAHs at remote sites has been mostly found in the submicrometer range (Lipiatou and



437 Saliot, 1991), also during the measurements reported here (own, unpublished data measured  
438 simultaneously). For particles of 0.5  $\mu\text{m}$  aerodynamic size  $v_{\text{dep}} \approx 0.1 \text{ cm s}^{-1}$  can be expected  
439 for the mean wind velocity at Selles Beach, i.e. 5  $\text{m s}^{-1}$ . Actually,  $v_{\text{dep}}$  is not very sensitive to  
440 wind speed for this particle size range. (Slinn and Slinn, 1980) Adopting  $v_{\text{dep}} = 0.1 \text{ cm s}^{-1}$   
441 would suggest  $F_{\text{p dep}} \approx -0.023, -0.016$  and  $-0.010 \mu\text{g m}^{-2} \text{ d}^{-1}$  for PHE, FLT and PYR ( $c_{\text{p}} = 0.26,$   
442  $0.19$  and  $0.11 \text{ ng m}^{-3}$ , respectively, mean of the same 5 day-time sampling intervals in the  
443 period 3-10 July for which  $F_{\text{c}}$  was determined, Table S5a). This means that the contribution of  
444  $F_{\text{p dep}}$  to dry deposition of PHE was negligible ( $F_{\text{p dep}} \approx 1000 \times F_{\text{p dep}}$ ;  $F_{\text{c}} = -26 \mu\text{g m}^{-2} \text{ d}^{-1}$ ) and  
445  $F_{\text{p dep}}$  negligibly compensated for net-volatilization of FLT and PYR in diffusive air-sea  
446 exchange ( $F_{\text{c}} = +0.91$  and  $+0.79 \mu\text{g m}^{-2} \text{ d}^{-1}$  for FLT and PYR, respectively). The mass median  
447 diameter of the semivolatile PAHs FLT and PYR might well be larger than 0.5  $\mu\text{m}$  as a  
448 consequence of redistribution in the aerosol along transport. However, even then, particle  
449 deposition could not have significantly compensated for net-volatilization, as for 1  $\mu\text{m}$   
450 particles  $F_{\text{p dep}}$  would be higher by approximately a factor of 3 (Slinn and Slinn, 1980). For  
451 PHE, FLT and PYR  $F_{\text{p dep}} = -0.021, -0.018$  and  $-0.009 \mu\text{g m}^{-2} \text{ d}^{-1}$ , respectively, were  
452 determined experimentally at Finokalia Observatory in 2001 (mean of 25 weeks between  
453 March and October; Tsapakis et al., 2006). This means that within measurement uncertainties  
454 the particle deposition fluxes found in 2012 are the same than one decade earlier, in both  
455 absolute and relative (3 PAH members) terms. These fluxes are also in agreement with what  
456 was estimated in the Aegean Sea in summer 2006, namely  $F_{\text{p dep}} = -0.010- -0.015 \mu\text{g m}^{-2} \text{ d}^{-1}$   
457 for the same PAHs based on assuming  $v_{\text{dep}} \approx 0.2 \text{ cm s}^{-1}$  (Castro-Jiménez et al., 2012).  
458 A similar calculation of for the BDEs for one day-time sampling interval ( $c_{\text{p}} = 0.16$  and  $0.20$   
459  $\text{ng m}^{-3}$  for BDE47 and BDE99, respectively, for day-time 6 July for which  $F_{\text{c}}$  was determined,  
460 Table S5b) suggests that the contribution of  $F_{\text{p dep}}$  to dry deposition of BDE47 was negligible,  
461 too ( $F_{\text{p dep}} \approx 100 \times F_{\text{p dep}}$ ;  $F_{\text{c}} = +3.0 \mu\text{g m}^{-2} \text{ d}^{-1}$ ), while no direct comparison can be made for



462 BDE99 ( $|F_c| \leq 3.8 \mu\text{g m}^{-2} \text{d}^{-1}$ ; Table S5b). Hereby,  $v_{\text{dep}} = 0.3 \text{ cm s}^{-1}$  was adopted to account  
463 for mass median diameters close to  $1 \mu\text{m}$  near the sources and mass transfer kinetic  
464 limitations for re-distribution during long-range transport (Cetin and Odabasi, 2008; Luo et  
465 al., 2014; and in agreement with own, unpublished data measured simultaneously in a short  
466 distance).

467 Significant vertical concentration differences in the particulate phase,  $\Delta c_p/\Delta z > 0$  and  $\Delta c_p/\Delta z$   
468  $< 0$ , were found. Notably during one day-time and sequential night-time sampling (6-7 July)  
469 and during day-time of 9 July all significant gradients determined for particulate phase  
470 contaminants were negative, i.e. higher concentrations at the lower level,  $z_1$  (PHE and FLT  
471 each 1, PYR 2 cases; PBDEs each 1 case; Table S3), while the opposite gradient was found in  
472 other nights and days. Apart from particle sources at the ground (not relevant here), vertical  
473 particle gradients may be sustained by turbulent diffusion (Pryor et al., 2008). While average  
474 wind speed was highest during day-time of 9 July, it was average during 6-7 July. No fluxes  
475 can be derived from the gradients determined in this study, downward or upward.

476

#### 477 **4. Conclusions**

478 The diurnal variation of contaminant concentrations in air at a remote coastal site in the  
479 Aegean Sea was explained by the combination of atmospheric mixing depth and volatilisation  
480 from the sea surface. Volatilisation from the sea surface has significantly contributed to the  
481 night-time maxima of PCB28. Apart from long-range transport across the Aegean Sea, local  
482 sources were indicated for PBDEs: PBDE cycling was characterized by volatilization and  
483 transport from the island during the day and deposition to the sea surface.

484 We successfully quantified the diffusive air-sea exchange flux of 4 3-4 ring PAHs (in the  
485 upper  $\text{pg m}^{-3}$  concentration range), 3 OCPs, 3 PCBs and 2 PBDEs (in the lower  $\text{pg m}^{-3}$   
486 concentration range) at a remote coastal site using a gradient in combination with the eddy



487 covariance technique. Many vertical gradients were insignificant and concentrations of other  
488 analytically targeted PAHs, PCBs, OCPs and PBDEs remained <LOQ. More substances could  
489 have been included using high-volume sampling, by which the sampled air volume could  
490 have been increased by one order of magnitude.

491 Both flux directions were observed (fluctuation) for the OCPs studied, as well as for 3 PAHs  
492 (ACE, FLT, PYR) and 1 PCB (PCB52), not determined by the day-night cycle. Fluctuation of  
493 more substances might have been hidden by the method's uncertainties. Hence, the mean flux  
494 direction on one hand side and observations during part of the time of the trace substances  
495 may differ. E.g. volatilisation of BDE47 (observed in 1 night only) may have been the  
496 exception. In general, longer observations and across seasons of the flux is needed to assess  
497 the state of air-sea exchange of those anthropogenic trace substances, which have been  
498 approaching phase equilibrium historically (Jantunen and Bidleman, 1995; Stemmler and  
499 Lammel, 2009; Berrojalbiz et al., 2014) or seasonally (Mulder et al., 2014).

500

#### 501 **Acknowledgements**

502 We thank Giorgos Kouvarakis and Nikolas Mihalopoulos, University of Crete, Iraklion, and  
503 Günter Schebeske, MPIC, for on-site support and Dušan Lago, MU, for air mass back-  
504 trajectory modelling. This research was supported by the Granting Agency of the Czech  
505 Republic (project No. 312334), the Czech Ministry of Education (LO1214), and the European  
506 Union FP7 under grant agreement n° 262254 (ACTRIS).

507

#### 508 **Supporting Information**

509 Detailed methodological information (substance properties, analytical quality assurance  
510 parameters, micrometeorological technique, two-box model) and results (meteorological  
511 situation, transfer velocity, atmospheric concentration and flux data).

512

#### 513 **References**

- 514 Allan, I.J., Booij, K., Paschke, A., Vrana, B., Mills, G.A., and Greenwood, R.: Field  
515 performance of seven passive sampling devices for monitoring of hydrophobic substances.  
516 *Environ. Sci. Technol.*, 43, 5383-5390, 2009.
- 517 Atlas, E., and Giam, C.S.: Sea-air exchange of high-molecular weight synthetic organic  
518 compounds. In: *The role of air-sea exchange in geochemical cycles* (Buat-Ménard, P.,  
519 ed.), NATO ASI Ser. Vol. C185, Reidel, Dordrecht, the Netherlands, pp. 295-329, 1986
- 520 Berrojalbiz, N., Castro-Jiménez, J., Mariani, G., Wollgast, J., Hanke, G., and Dachs, J.:  
521 Atmospheric occurrence, transport and deposition of polychlorinated biphenyls and  
522 hexachlorobenzene in the Mediterranean and Black Seas. *Atmos. Chem. Phys.*, 14, 8947-  
523 8959, 2014.



- 524 Bidleman, T.F., and McConnell, L.L.: A review of field experiments to determine air–water  
525 gas-exchange of persistent organic pollutants. *Sci. Total Environ.*, 159, 101-107, 1995.
- 526 Booij, K., and Smedes, F.: An improved method for estimating in situ sampling rates of  
527 nonpolar passive samplers. *Environ. Sci. Technol.*, 44, 6789–6794, 2010.
- 528 Borgå, K., Gabrielsen, G.W., and Skaare, J.U.: Biomagnification of organochlorines along a  
529 Barents Sea food chain. *Environ. Pollut.*, 113, 187-198, 2001.
- 530 Bruhn, R., Lakaschus, S., and McLachlan, M.S.: Air/sea gas exchange of PCBs in the  
531 southern Baltic sea. *Atmos. Environ.*, 37, 3445–3454, 2003.
- 532 Castro-Jiménez, J., Berrojalbiz, N., Wollgast, J., and Dachs, J.: Polycyclic aromatic  
533 hydrocarbons (PAHs) in the Mediterranean Sea: Atmospheric occurrence, deposition and  
534 decoupling with settling fluxes in the water column. *Environ. Pollut.*, 166, 40-47, 2012.
- 535 Cetin, B., and Odabasi, M.: Atmospheric concentrations and phase partitioning of  
536 polybrominated diphenyl ethers (PBDEs) in Izmir, Turkey. *Chemosphere*, 71, 1067-1078,  
537 2008.
- 538 Doskey, P.V., Kotamarthi, V.R., Fukui, Y., Cook, D.R., Breitbeil, F.W., and Wesely, M.L.:  
539 Air-surface exchange of peroxyacetyl nitrate at a grassland site. *J. Geophys. Res.*, 109,  
540 D10310, 2004.
- 541 Else, B.G.T., Papakyriakou, T.N., Granskog, M.A., and Yackel, J.J.: Observations of sea  
542 surface  $f_{CO_2}$  distributions and estimated air–sea  $CO_2$  fluxes in the Hudson Bay region  
543 (Canada) during the open water season. *J. Geophys. Res.*, 113, C08026, 2004.
- 544 Gigliotti, C.L., Brunciak, P.A., Dachs, J., Glenn, T.R., Nelson, E.D., Totten, L.A., and  
545 Eisenreich, S.J.: Air-water exchange of polycyclic aromatic hydrocarbons in  
546 theNewYork-NewJersey, USA, harbor estuary. *Environ. Toxicol. Chem.*, 21, 235-244,  
547 2002.
- 548 Halse, A.K., Schlabach, M., Eckhardt, S., Sweetman, A.J., Jones, K.C., and Breivik, K.:  
549 Spatial variability of POPs in European background air. *Atmos. Chem. Phys.*, 11, 1549–  
550 1564, 2011.
- 551 Jantunen, L.M., and Bidleman, T.F.: Reversal of the air-water gas-exchange direction of  
552 hexachlorocyclohexanes in the Bering and Chukchi Seas: 1993 vs. 1988, *Environ. Sci.*  
553 *Technol.*, 29, 1081-1089, 1995.
- 554 Kamarianos, A., Karamanlis, X., and Galoupi, E.: Pollution of coastal areas of N. Greece by  
555 organochlorine pesticides and polychlorinated biphenyls (PCBs). In: Proceedings of the  
556 1st Environmental Conference of Macedonia, 1–4 March 2002, Thessaloniki, Greece, pp.  
557 116–121, 2002.
- 558 Keyte I.J., Harrison R.M., and Lammel G.: Chemical reactivity and long-range transport  
559 potential of polycyclic aromatic hydrocarbons – a review. *Chem. Soc. Rev.*, 42, 9333-  
560 9391, 2013.
- 561 Kouvarakis, G., Tsigaridis, K., Kanakidou, M., and Mihalopoulos, N.: Temporal variations of  
562 surface regional background ozone over Crete Island in the southeast Mediterranean. *J.*  
563 *Geophys. Res.*, 105, 4399-4407, 2000.
- 564 Kurt-Karakus, P.B., Bidleman, T.F., Staebler, R.M., and Jones, K.C.: Measurement of DDT  
565 fluxes from a historically treated agricultural soil in Canada, *Environ. Sci. Technol.*, 40,  
566 4578-4585, 2006.
- 567 Lakaschus, S., Weber, K., Wania, F., and Schrems, O.: The air-sea equilibrium and time trend  
568 of hexachlorocyclohexanes in the Atlantic Ocean between the Arctic and Antarctica,  
569 *Environ. Sci. Technol.*, 36, 138– 145, 2002.
- 570 Lammel, G., Brüggemann, E., Müller, K., and Röhr, A.: On the horizontal homogeneity of  
571 mass-related aerosol properties, *Environ. Monitoring Assessment*, 84, 265-273, 2003.
- 572 Lammel, G., Klánová, J., Ilić, P., Kohoutek, J., Gasić, B., Kovacić, I., Lakić, N., and Radić,  
573 R.: Polycyclic aromatic hydrocarbons on small spatial and temporal scales – I. Levels and  
574 variabilities. *Atmos. Environ.*, 44, 5015-5021, 2010.



- 575 Lammel, G., Klánová, J., Erić, L., Ilić, P., Kohoutek, J., and Kovacić, I.: Sources of  
576 organochlorine pesticides in an urban Mediterranean environment: Volatilisation from  
577 soil, *J. Environ. Monit.*, 13, 3358–3364, 2011.
- 578 Lammel, G., Audy, O., Besis, A., Efstathiou, C., Eleftheriadis, K., Kohoutek, J., Kukučka, P.,  
579 Mulder, M.D., Příbylová, P., Prokeš, R., Rusina, T., Samara, C., Sofuoglu, A., Sofuoglu,  
580 S.C., Tasdemir, Y., Vassilatou, V., Voutsas, D., and Vrana B.: Air and seawater pollution  
581 and air-sea exchange of persistent organic pollutants in the Aegean Sea: spatial trends of  
582 PAHs, PCBs, OCPs and PBDEs. *Environ. Sci. Pollut. Res.*, 22, 11301-11313, 2015.
- 583 Lee, R.G.M., Hung, H., Mackay, D., and Jones, K.C.: Measurement and modeling of the  
584 diurnal cycling of atmospheric PCBs and PAHs. *Environ. Sci. Technol.*, 32, 2172-2179,  
585 1998.
- 586 Lipiatou, E., Saliot, A.: Fluxes and transport of anthropogenic and natural polycyclic  
587 aromatic-hydrocarbons in the western Mediterranean Sea. *Mar. Chem.*, 32, 51-71., 1991.
- 588 Lohmann, R., Dapsis, M., Morgan, E.J., Dekany, E., and Luey, P.J.: Determining air-water  
589 exchange spatial and temporal trends of freely dissolved PAHs in an urban estuary using  
590 passive polyethylene samplers. *Environ. Sci. Technol.*, 45, 2655-2662, 2011.
- 591 Lohmann, R., Booij, K., Smedes, F., and Vrana, B.: Use of passive sampling devices for  
592 monitoring and compliance checking of POP concentrations in water. *Environ. Sci. Pollut.*  
593 *Res.*, 19, 1885–95, 2012.
- 594 Luo, P., Ni, H.G., Bao, L.J., Li, S.M., and Zeng, E.Y.: Size distribution of airborne particle-  
595 bound polybrominated diphenyl ethers and its implications for dry and wet deposition.  
596 *Environ. Sci. Technol.*, 48, 13793-13799, 2014.
- 597 Majewski, M.S., Desjardins, R., Rochette, P., Pattey, E., Seiber, J., and Glotfelty, D.E.: Field  
598 comparison of an eddy accumulation and an aerodynamic-gradient system for measuring  
599 pesticide volatilization fluxes. *Environ. Sci. Technol.*, 27, 121-128, 1993.
- 600 Mandalakis, M., and Stephanou, E.G.: Study of atmospheric PCB concentrations over eastern  
601 Mediterranean Sea. *J. Geophys. Res.*, 107, 4716, 2002.
- 602 Mandalakis, M., Apostolaki, M., Stephanou, E.G., and Stavrakakis, S.: Mass budget and  
603 dynamics of polychlorinated biphenyls in the east Mediterranean Sea. *Glob. Biogeochem.*  
604 *Cycles*, 19, GB3018, 2005.
- 605 Melymuk, L., Bohlin-Nizzetto, P., Prokeš, R., Kukučka, P., and Klánová, J.: Sampling  
606 artifacts in active air sampling of semivolatile organic contaminants: Comparing  
607 theoretical and measured artifacts and evaluating implications for monitoring networks.  
608 *Environ. Pollut.* doi:10.1016/jenvpol.2015.12.015, 2016.
- 609 Mihalopoulos, N., Stephanou, E., Pilitsidis, S., Kanakidou, M., and Bousquet, P.:  
610 Atmospheric aerosol composition above the Eastern Mediterranean region. *Tellus B*, 49,  
611 314-326, 1997.
- 612 Mulder, M.D., Heil, A., Kukučka, P., Klánová, J., Kuta, J., Prokeš, R., Sprovieri, F., and  
613 Lammel, G.: Air-sea exchange and gas-particle partitioning of polycyclic aromatic  
614 hydrocarbons in the Mediterranean. *Atmos. Chem. Phys.*, 14, 8905–8915, 2014.
- 615 Mulder, M.D., Heil, A., Kukučka, P., Kuta, J., Příbylová, P., Prokeš, R., and Lammel, G.:  
616 Long-range atmospheric transport of PAHs, PCBs, OCPs and PBDEs to the central and  
617 eastern Mediterranean 2010. *Atmos. Environ.*, 111, 51-59, 2015.
- 618 Parmele, L.H., Lemon, E.R., and Taylor, A.W.: Micrometeorological measurement of  
619 pesticide vapor flux from bare soil and corn under field conditions. *Water Air Soil Pollut.*,  
620 1, 433-451, 1972.
- 621 Perlinger, J.A., Tobias, D.E., Morrow, P.S., and Doskey, P.V.: Evaluation of novel techniques  
622 for measurement of air-water exchange or persistent bioaccumulative toxicants in Lake  
623 Superior. *Environ. Sci. Technol.*, 39, 8411-8419, 2005.



- 624 Rowe, M.D., and Perlinger, J.A.: Micrometeorological measurement of hexachlorobenzene  
625 and polychlorinated biphenyl compound air-water gas exchange in Lake Superior and  
626 comparison to model predictions. *Atmos. Chem. Phys.*, 12, 4607-4617, 2012.
- 627 Rusina, T., Smedes, F., Koblížková, M., and Klánová, J.: Calibration of silicone rubber  
628 passive samplers: experimental and modeled relations between sampling rate and  
629 compound properties. *Environ. Sci. Technol.*, 44, 362-367, 2010a.
- 630 Rusina, T., Smedes, F., and Klanova, J.: Diffusion coefficients of polychlorinated biphenyls  
631 and polycyclic aromatic hydrocarbons in polydimethylsiloxane and low-density  
632 polyethylene polymers. *J. Appl. Polymer Sci.*, 116, 1803-1810, 2010b.
- 633 Sandy, A.L., Guo, J., Miskewitz, R.J., McGillis, W.R., and Rodenburg, L.A.: Fluxes of  
634 polychlorinated biphenyls volatilizing from the Hudson River, New York measured using  
635 micrometeorological approaches. *Environ. Sci. Technol.*, 46, 885-891, 2012.
- 636 Schwarzenbach, R.P., Gschwend, P.M., and Imboden, D.M.: *Environmental Organic*  
637 *Chemistry*, 2<sup>nd</sup> ed., Wiley, Hoboken, USA, 2003.
- 638 Slinn, S.A., and Slinn, W.G.N.: Predictions for particle deposition on natural waters. *Atmos.*  
639 *Environ.*, 14, 1013-1016, 1980.
- 640 Smedes, F.: Monitoring of chlorinated biphenyls and polycyclic aromatic hydrocarbons by  
641 passive sampling in concert with deployed mussels. In: *Passive sampling techniques in*  
642 *Environmental Monitoring (Comprehensive Analytical Chemistry Vol. 48; Greenwood,*  
643 *R., Mills, G., Vrana, B., eds.), pp. 407-448, Elsevier, Amsterdam, the Netherlands, 2007.*
- 644 Stemmler, I., and Lammel, G.: Cycling of DDT in the global oceans 1950-2002: World ocean  
645 returns the pollutant. *Geophys. Res. Lett.*, 36, L24602, 2009.
- 646 Stohl, A., Hittenberger, M., and Wotawa, G.: Validation of the Lagrangian particle dispersion  
647 model FLEXPART against large scale tracer experiments. *Atmos. Environ.*, 32, 4245-  
648 4264, 1998.
- 649 Tasdemir, Y., and Esen, F.: Dry deposition fluxes and deposition velocities of PAHs at an  
650 urban site in Turkey. *Atmos. Environ.*, 41, 1288-1301, 2007.
- 651 Tsapakis, M., and Stephanou, E.G.: Polycyclic aromatic hydrocarbons in the atmosphere of  
652 the Eastern Mediterranean. *Environ. Sci. Technol.*, 39, 6584-6590, 2005.
- 653 Tsapakis, M., and Stephanou, E.G.: Diurnal cycle of PAHs, nitro-PAHs and oxy-PAHs in a  
654 high oxidation capacity marine background atmosphere. *Environ. Sci. Technol.*, 41, 8011-  
655 8017, 2007.
- 656 Tsapakis M., Apostolaki, M., Eisenreich, S., and Stephanou, E.G.: Atmospheric deposition  
657 and marine sediment fluxes of polycyclic aromatic hydrocarbons in the east  
658 Mediterranean Basin. *Environ. Sci. Technol.* 40, 4922-4927, 2006.
- 659 UNEP-GEMS - United Nations Environment Programme Global Environment Monitoring  
660 System: Water Programme, annual report, Geneva, 2006.
- 661 Voegelezang, D.H.P., and Holtslag, A.A.M.: Evaluation and model impacts of alternative  
662 boundary-layer height formulations. *Bound. Layer Met.*, 81, 245-269, 1996.
- 663 Williams, R.M.: A model for the dry deposition of particles to natural water surfaces. *Atmos.*  
664 *Environ.*, 16, 1933-1938, 1982.
- 665 Wong, F., Jantunen, L.M., Papakyriakou, T., Staebler, R.M., Stern, G.A., and Bidleman, T.F.:  
666 Comparison of micrometeorological and two-film estimates of air-water gas exchange for  
667  $\alpha$ -hexachlorocyclohexane in the Canadian Archipelago. *Environ. Sci. Pollut. Res.*, 19,  
668 1908-1914, 2012.
- 669 Zhang, L.M., Cheng, I., Wu, Z.Y., Harner, T., Schuster, J., Charland, J.P., Muir, D., and  
670 Parnis, J.M.: Dry deposition of polycyclic aromatic compounds to various land covers in  
671 the Athabasca oil sands region. *J. Adv. Model. Earth Syst.*, 7, 1339-1350, 2015.
- 672 Zhou, S., Lee, A.K.Y., McWhinney, R.D., and Abbatt, J.P.D.: Burial effects of organic  
673 coatings on the heterogeneous reactivity of particle-borne benzo(a)pyrene (BaP) towards  
674 ozone. *J. Phys. Chem. A*, 116, 7050-7055, 2012.



675 Table 1. Statistics of (a) concentrations at ground level,  $z_1 = 1.05$  m and (b) vertical gradients,  
 676  $\Delta c_z$ , over  $\Delta z = 1.75$  m of gaseous PAHs and halogenated POPs. Mean  $\pm$  standard deviation (n,  
 677 min-max),  $\text{ng m}^{-3}$ , except PBDEs:  $\text{pg m}^{-3}$ ). All data included (exceeding or below uncertainty  
 678 thresholds), individual data: see Tables S3, S4. For mean and standard deviations values  
 679  $<$ LOQ were replaced by LOQ/2.

680 a.

	all samples	night-time	day-time
ACE	0.091 $\pm$ 0.021 (0.059–0.12)	0.11 $\pm$ 0.006 (5, 0.11–0.12)	0.076 $\pm$ 0.012 (5, 0.059–0.091)
PHE	1.28 $\pm$ 0.89 (0.21–3.54)	1.00 $\pm$ 0.52 (8, 0.21–1.46)	1.47 $\pm$ 1.10 (10, 0.25–3.54)
FLT	0.35 $\pm$ 0.26 (0.044–0.89)	0.29 $\pm$ 0.24 (8, 0.046–0.76)	0.40 $\pm$ 0.29 (10, 0.044–0.89)
PYR	0.23 $\pm$ 0.20 (0.09–0.86)	0.18 $\pm$ 0.09 (6, 0.13–0.34)	0.28 $\pm$ 0.25 (8, 0.09–0.86)
PCB 28	0.020 $\pm$ 0.009 (0.006–0.037)	0.021 $\pm$ 0.010 (5, 0.008–0.033)	0.020 $\pm$ 0.009 (10, 0.006–0.037)
PCB 52	0.012 $\pm$ 0.007 (0.003–0.024)	0.014 $\pm$ 0.008 (6, 0.003–0.024)	0.011 $\pm$ 0.005 (10, 0.003–0.023)
PCB101	0.008 $\pm$ 0.002 (0.005–0.011)	0.009 $\pm$ 0.002 (4, 0.006–0.011)	0.006 $\pm$ 0.001 (5, 0.005–0.008)
$\alpha$ -HCH	0.038 $\pm$ 0.021 (0.008–0.078)	0.056 $\pm$ 0.013 (6, 0.039–0.076)	0.031 $\pm$ 0.020 (10, 0.008–0.078)
$\gamma$ -HCH	0.106 $\pm$ 0.072 (0.007–0.245)	0.136 $\pm$ 0.078 (8, 0.030–0.245)	0.089 $\pm$ 0.067 (11, 0.007–0.242)
<i>p,p'</i> -DDE	0.007 $\pm$ 0.004 (0.003–0.015)	0.008 $\pm$ 0.003 (4, 0.006–0.012)	0.007 $\pm$ 0.004 (8, 0.003–0.015)
BDE 47	0.327 $\pm$ 0.119 (0.20–0.51)	0.265 $\pm$ 0.046 (3, 0.228–0.317)	0.36 $\pm$ 0.14 (5, 0.20–0.51)
BDE 99	0.218 $\pm$ 0.062 (0.14–0.31)	0.195 $\pm$ 0.024 (4, 0.161–0.214)	0.234 $\pm$ 0.077 (5, 0.137–0.313)

681

682

b.

	all samples	night-time	day-time
ACE	0.008 $\pm$ 0.047 (-0.026–0.10)	-0.001 $\pm$ 0.027 (4, -0.024–0.037)	0.019 $\pm$ 0.072 (3, -0.026–0.10)
PHE	1.24 $\pm$ 2.10 (-0.047–7.35)	1.19 $\pm$ 1.96 (4, -0.047–5.55)	1.29 $\pm$ 2.32 (6, 0.009–7.35)
FLT	0.19 $\pm$ 0.43 (-0.46–0.95)	0.33 $\pm$ 0.44 (6, -0.25–0.95)	0.073 $\pm$ 0.40 (6, -0.46–0.73)
PYR	0.081 $\pm$ 0.21 (-0.42–0.45)	0.18 $\pm$ 0.17 (6, 0.038–0.45)	0.004 $\pm$ 0.22 (6, -0.42–0.32)
PCB 28	0.024 $\pm$ 0.046 (-0.013–0.155)	0.013 $\pm$ 0.040 (7, -0.011–0.103)	0.032 $\pm$ 0.050 (10, -0.013–0.155)
PCB 52	0.016 $\pm$ 0.036 (-0.011–0.120)	0.009 $\pm$ 0.036 (7, -0.011–0.089)	0.020 $\pm$ 0.038 (10, -0.004–0.120)
PCB101	0.012 $\pm$ 0.018 (-0.005–0.044)	0.007 $\pm$ 0.019 (4, -0.005–0.035)	0.018 $\pm$ 0.018 (4, -0.001–0.044)
$\alpha$ -HCH	0.079 $\pm$ 0.188 (-0.048–0.675)	0.025 $\pm$ 0.131 (5, -0.048–0.258)	0.107 $\pm$ 0.212 (10, -0.019–0.675)
$\gamma$ -HCH	0.107 $\pm$ 0.273 (-0.159–0.890)	0.018 $\pm$ 0.222 (7, -0.159–0.510)	0.164 $\pm$ 0.297 (11, -0.073–0.890)
<i>p,p'</i> -DDE	0.001 $\pm$ 0.005 (-0.006–0.009)	0.002 $\pm$ 0.004 (4, -0.001–0.007)	0.001 $\pm$ 0.006 (5, -0.006–0.009)
BDE 47	-0.229 $\pm$ 0.072 (-0.280–0.178)	n.d.	-0.229 $\pm$ 0.072 (2, -0.280–0.178)
BDE 99	-0.042 $\pm$ 0.017 (-0.059–0.025)	-0.058 (1)	-0.034 $\pm$ 0.014 (2, -0.044–0.025)

683





684 Table 2. Concentrations in air (gaseous, ground level,  $z = 1.05$  m, if >LOQ for most samples)  
685 ( $\text{ng m}^{-3}$ , except PBDEs:  $\text{pg m}^{-3}$ ) and surface seawater ( $\text{pg L}^{-1}$ ) and fugacity ratios,  $f_a/f_w$ .

	$c_a$	$c_w$	$f_a/f_w$
FLT	0.35	18.2	19
PYR	0.23	4.4	59
PCB 28	0.020	4.65	0.15
PCB 52	0.012	0.54	0.94
PCB 101	0.0076	0.84	0.34
<i>p,p'</i> -DDE	0.0072	0.84	0.76
BDE 47	0.33	0.15	2600
BDE 99	0.22	0.038	16140

686



687 Figure captions

688

689 Fig. 1. Gaseous (a) PAH and (b) halogenated substances' concentrations at ground level,  $z_1 =$   
690 1.05 m (upper), vertical concentration differences,  $\Delta c_z = c_{z2} - c_{z1}$ , over  $\Delta z = 1.75$  m (middle)  
691 and vertical fluxes,  $F_c = -v_{tr} \Delta c_z$  (positive = upward, negative = downward; lower). Only  
692 significant data (exceeding uncertainty thresholds) shown, gaps = no data.

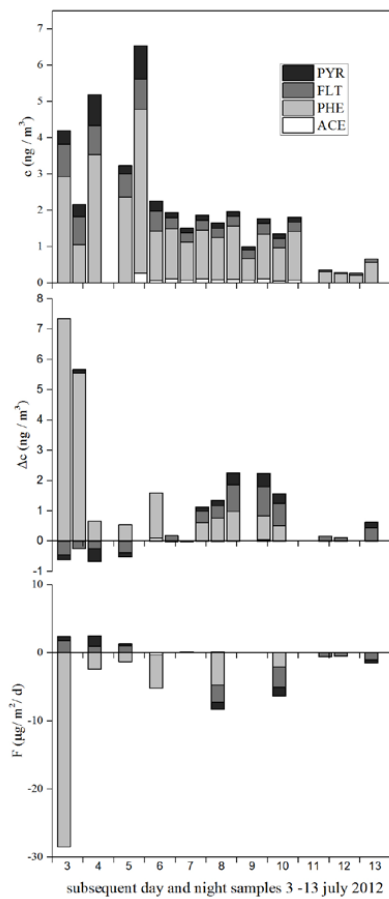
693

694 Fig. 2. Predicted and observed concentrations of selected contaminants, (a) PCB28, (b) FLT  
695 and (c) BDE47 during 6-10 July 2012.

696

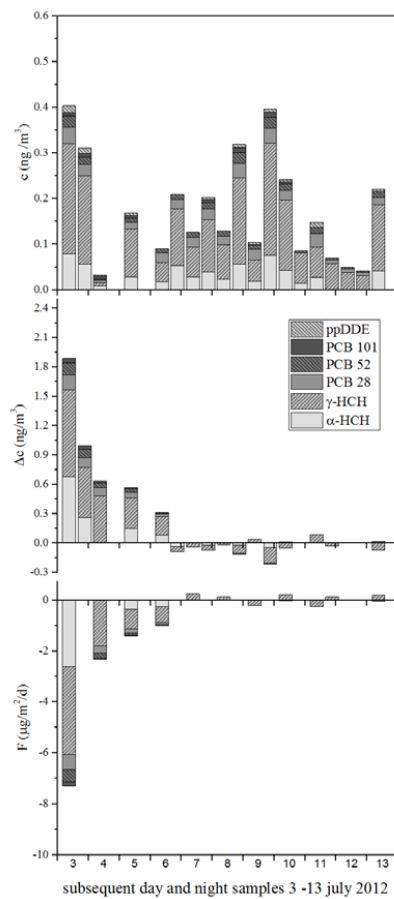


697 Fig. 1  
698 a.



699  
700

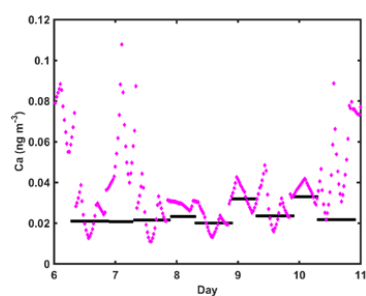
b.



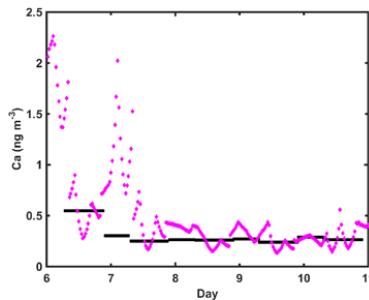


701 Fig. 2.

702 a.

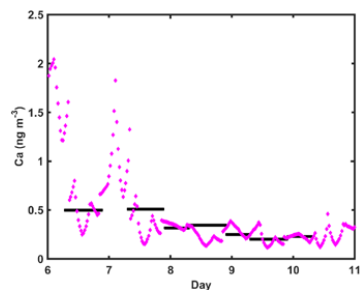


b.



703  
704

c.



705  
706